

INVESTIGATION OF MIXED-MODE FRACTURE BY SMEARED CRACK MODEL WITH EMBEDDED CRACK BAND

Mochammad Afifuddin^{*1}, Zhishen Wu^{*2}, Atsuhiko Machida^{*3}, Matsumura Takuro^{*4}

1. Introduction: In finite element analysis of concrete structures, cracks have been represented in a discrete or smeared fashion. Due to the simple conception and easy implementation in a general purpose finite element program for smeared crack models, the discrete crack models were rapidly replaced by smeared crack models. Although these models have been widely used in the analysis of fracture, they still suffer from a number of shortcomings. Rots[1] has applied different smeared crack models to cases of localized fracture and has demonstrated three problems of smeared crack models, namely, directional bias, spurious kinematics modes, and stress locking. On the other hand, smeared crack models seem to overestimate the stiffness and strength of structures that exhibits shear-dominated behavior [2]. The aim of this paper is to examine the behavior of the failure prediction of smeared crack model based on the fracture energy related softening. Numerical simulation are shown for three point bending specimens and four point shear specimens. The reason of shortcoming of smeared crack models is discussed. The size effect is also investigated.

2. Formulation of Constitutive Relation: A constitutive relation for the fracture process zone (FPZ) as shown in Figure 1 is selected to nonlinear model and time independent fracture.

$$\sigma = \zeta(v) = b[a + (v + v^*)^{1/2}] \exp[-c(v + v^*)^{1/2}] \dots (1)$$

in which: a, b, c and v^* are decided uniquely by:

$$\sigma = \zeta(0) = f_t \dots (1.a); \int_0^\infty \sigma dv = G_f \dots (1.b)$$

$$\left. \frac{d\sigma}{dv} \right|_{v=0} = H_0 \dots (1.c); \sigma = \zeta(-v^*) = \alpha f_t \dots (1.d)$$

where f_t , G_f and H_0 are: tensile strength, fracture energy and initial slope of $\sigma-v$ curve. α is a constant value of 0.5 ~ 0.9. If the hardening effect of concrete before strength in the fracture process zone is considered, then $H_0 \rightarrow +\infty$ and $v^* = 0$. In this study, a crack band model embedded in a fixed smeared crack concept is adopted as shown in Figure 2. Therefore, the relationship between the crack displacement v and the fracturing strain ϵ can be expressed as:

$$dv = d\epsilon_f h \dots (2)$$

The relation between the local and global stress increment can be related by using the transformation matrix $T(\theta)$.

$$\Delta \sigma_{nl} = T(-\theta)^T \Delta \sigma, T(\theta) = \begin{bmatrix} c^2 & s^2 & cs \\ s^2 & c^2 & -cs \\ -2cs & 2cs & c^2 - s^2 \end{bmatrix} \dots (3)$$

where $c = \cos \theta$, $s = \sin \theta$, and θ is the angle between the global coordinate axes and the axes aligned with the direction of cracking. After using the transformation matrix, the relation between the local fracture strain increment $\Delta \epsilon_f$ and the global total strain increment $\Delta \epsilon$ can be derived as:

$$\Delta \epsilon_f = (T(-\theta)^T D_c T(-\theta) + D_f)^{-1} [T(-\theta)^T D_c (\Delta \epsilon)] \dots (4)$$

Finally, we obtain a general global constitutive equation:

$$\Delta \sigma = D_c [I - T(-\theta)(T(-\theta)^T D_c T(-\theta)^T + D_f)^{-1} T(-\theta)^T D_c] \Delta \epsilon \dots (5)$$

where D_c = elastic stiffness matrix, $D_f = \text{diag}[H', \lambda E_c, \beta G_c]$, $H' = \partial \sigma / \partial v$, E_c = elastic young's modulus, G_c = elastic shear modulus, λ = effectiveness factor customarily used in the crack band model and introduced to consider the deterioration of the compressive strength and stiffness of concrete in the direction normal to the cracks. If $\lambda \rightarrow \infty$, no deterioration is considered. β = shear reduction factor. The shear modulus βG_c is used to model the decreasing shear stiffness and the aggregate interlock in unreinforced materials.

3. Numerical Studies and Results

3.1. Three Point Bending Fracture: Mode I fracture of Three-point bending (TPB) beams were first analyzed. Three different sizes are considered ($b=7.874$; 15.748 ; and 31.496 inch) and the width was held constant at 1 inch. The notch length to beam-depth ratio, a_0/b , was varied from 0 to 0.5. Shown in Figure 3 is the finite element mesh of TPB specimen. Typical resultant curve for TPB fracture specimen ($b=31.496$ inch) are shown in Figure 4. For deep initial notched, stiffness and loading capacity decreases, whereas ductility increases. The size effect is

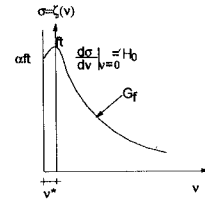


Figure 1. $\sigma-v$ Curve

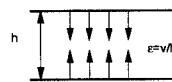


Figure 2. Crack Band Embedded

^{*1} Graduate Student, Graduate School of Science and Engineering, Saitama University

^{*2} Department of Urban and Civil Engineering, Ibaraki University

^{*3} Department of Civil and Environmental Engineering, Saitama University

^{*4} Central Research Institute of Electric Power Industry, Chiba

illustrated in Figure 5. It can be seen that the significant size effect appears in the investigated range of sizes for different initial notch depths. With growing size the nominal ultimate stress is decreasing. Slope of softening of unnotched beam seem to be the envelope of notched beam. However, the numerical calculation in the case of unnotched beams seem to become instable even in the numerical algorithm of arch length method.

3.2. Fracture of Four-Point Shear (FPS) Specimens: The main aim of this study is to examine if the smeared crack approach can be used to model the mixed mode fracture, especially for the shear dominated behavior of concrete structures. For this purpose, the simulation of shear

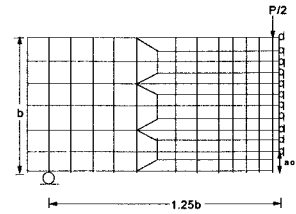


Figure 3. FEM. mesh of TPB specimen

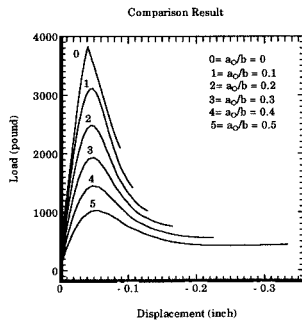


Figure 4. Load-Displacement Curve

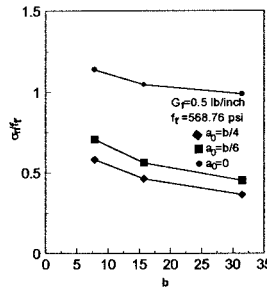


Figure 5. Size Effect for TPB

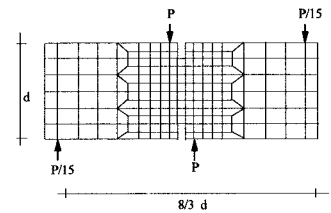


Figure 6. FEM. mesh of FPS specimen

failure of FPS beams is carried here (Figure 6). Four different sizes are considered ($b=3, 6, 8$, and 12 inch). The notch length to beam depth ratio was varied $d/3$ and $d/6$. Size effect for FPS specimens is shown in Figure 7. It is quite similar with the result of TPB specimens. The predicted crack pattern for specimen ($b=8$ inch) is compared with experimental result [3] is shown in Figure 8. The crack propagation is expressed well by the model. However in numerical calculations, it is realized that the element with smeared crack representation seem to be incapable of representing the sliding mode at the element level. By considering the opening and sliding modes (Fig. 9), if crack is fully open, the opening mode is indicated to a zero energy mode. However, even the shear stiffness dropped to zero, the sliding mode is not show a zero energy model. This should be the source of the major deficiencies of smeared crack models. Due to this reasons the stiffness and strength of structures should be overestimated by smeared crack models.

4. Conclusion: By numerical calculations, it is found that smeared crack model enables a modeling of the size effect in cases of tension and shear failure in quasibrittle structures. However, smeared crack models failure to express the sliding mode in the cracked element and seem to overestimate the stiffness and strength of structures that exhibit shear dominated behavior.

References: 1. Rots, J.G., 'Computational Modeling of Concrete Fracture', Doctoral Thesis, Delft University, 1988.

2. Wu, Z., Afifuddin, M., et al., 'Prediction of Shear Dominated Behavior of Quasibrittle Structures by Smeared Crack Model', EASEC-5, 1995 (will be published).

3. Swartz, S.E., Taha, N.M., 'Crack Propagation and Fracture of Plain Concrete Beams Subjected to Shear and Compression', ACI Structural Journal, March, 1991

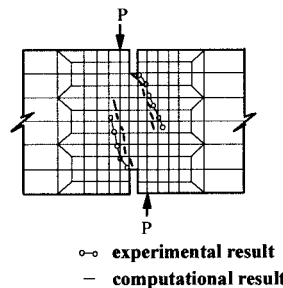


Figure 8. Crack Pattern

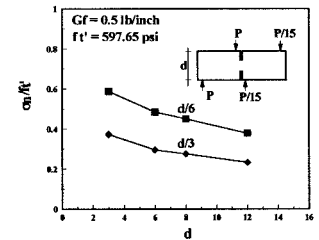


Figure 7. Size Effect for FPS

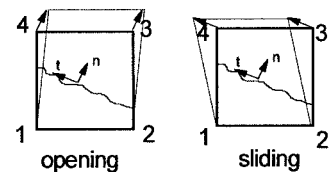


Figure 9. Cracked Element